Physica Medica 29 (2013) 436–446

Contents lists available at SciVerse ScienceDirect

Physica Medica

journal homepage: http://www.physicamedica.com

Original paper

# Evaluation of performance of an accelerator-based BNCT facility for the treatment of different tumor targets

M.S. Herrera [a,b,c,*], S.J. González [a,b], D.M. Minsky [a,b,c], A.J. Kreiner [a,b,c]

[a] Gerencia de Investigación y Aplicaciones, CNEA, Av. Gral. Paz 1499, B1650KNA Buenos Aires, Argentina
[b] Consejo Nacional de Investigaciones Científicas y Técnicas, Av. Rivadavia 1917, C1033AAJ Buenos Aires, Argentina
[c] Escuela de Ciencia y Tecnología, UNSAM, M. de Irigoyen 3100, B1650KNA Buenos Aires, Argentina

ARTICLE INFO

*Article history:*
Received 19 November 2012
Received in revised form
24 January 2013
Accepted 28 January 2013
Available online 23 February 2013

*Keywords:*
Accelerator-based neutron source
Treatment planning assessment
Whole-body dose assessment

ABSTRACT

*Purpose:* Encouraging Boron Neutron Capture Therapy (BNCT) clinical results obtained in recent years have stimulated intense research to develop accelerator-based neutron sources to be installed in clinical facilities. In this work an assessment of an accelerator-based BNCT facility for the treatment of different tumor targets was performed, comparing the accelerator-derived results with reported reactor-based trials under similar conditions and subjected to the same clinical protocols.
*Materials and methods:* A set of real image studies was used to cover clinical-like cases of brain and head-and-neck tumors. In addition, two clinical cases of malignant nodular melanoma treated at the RA-6 BNCT facility in Argentina were used to thoroughly compare the clinical dosimetry with the accelerator-derived results.
*Results:* The minimum weighted dose delivered to the clinical target volume was higher than 30 Gy and 14 Gy for the brain tumor and head-and-neck cases, respectively, in agreement with those achieved in clinical applications. For the melanoma cases, the minimum tumor doses were equal or higher than those achieved with the RA-6 reactor for identical field orientation and protocol. The whole-body dose assessment showed that the maximum photon-equivalent doses for those normal organs close to the beam direction were below the upper limits considered in the protocols used in the present work.
*Conclusions:* The obtained results indicate not only the good performance of the proposed beam shaping assembly design associated to the facility but also the potential applicability of accelerator-based BNCT in the treatment of both superficial and deep-seated tumors.


## Introduction

Boron Neutron Capture Therapy (BNCT) has been mainly used in patients for which there is no solution using conventional means. The first clinical application of Boron Neutron Capture Therapy was implemented in the '50s to treat patients with brain tumors (glioblastoma multiforme) conducted at the Massachusetts General Hospital and the Brookhaven National Laboratory [1]. This particular radiation therapy, which is considered a targeted therapy, is based on the combined use of slow neutrons and one of the two stable isotopes of boron ($^{10}$B) to destroy tumor cells via the neutron capture reaction, $^{10}$B(n,α)$^{7}$Li. The selectivity of the therapy is based on the fact that only tumor cells containing $^{10}$B will be destroyed, leaving normal tissues preserved due to their low affinity with the boron drug. Over the years, improvements in boron compounds and neutron sources evidenced promising results that promoted the continuity of ongoing research and creation of new clinical protocols in several countries [2–6]. Main clinical targets include high-grade gliomas, metastatic and cutaneous melanomas, head-and-neck tumors, among others. Although to date BNCT clinical trials have been based on existing nuclear reactors as neutron sources, accelerators are preferred as an alternative to reactors because of their much lower cost and level of complexity and mainly due to the possibility of setting up these facilities in hospitals. From a neutronic point of view, the endothermic $^{7}$Li(p,n)$^{7}$Be nuclear reaction seems to be a fairly promising for accelerator-based BNCT since the reaction leads to a high neutron production and a fairly soft low-energy neutron spectrum. Nevertheless, other reactions such as $^{9}$Be(p,n)$^{9}$B, $^{9}$Be(d,n)$^{10}$B and $^{13}$C(d,n)$^{14}$N can be used to produce acceptable neutron fields [7–11]. At present, there are several research groups around the world planning to install electrostatic or electrodynamic accelerators in clinical facilities in order to develop accelerator-based neutron sources for BNCT. In particular, an accelerator-based

* Corresponding author. Gerencia de Investigaci\'on y Aplicaciones, CNEA, Av. Gral. Paz 1499, B1650KNA Buenos Aires, Argentina. Tel.: +54 11 67727103.
*E-mail address:* herrera@tandar.cnea.gov.ar (M.S. Herrera).

1120-1797/$ – see front matter 
http://dx.doi.org/10.1016/j.ejmp.2013.01.006

BNCT facility is being constructed at the Ibaraki-prefecture in Japan. In this case, the technology choice is the combination of an 8 MeV (~10 mA) proton Linac consisting of a radio frequency quadrupole (RFQ) and a drift tube linac (DTL) and a beryllium target [12]. For this project, the Japanese group is developing a treatment planning system, patient setting device and monitors, among others [13]. Also in Japan, at Kyoto University Research Institute, the cyclotron HM-30 accelerator manufactured by Sumitomo Heavy Industries has been reconditioned to be used in the therapy. A beam shaping assembly to filter and moderate the fast neutrons emitted from the $^{9}$Be(p,n) nuclear reaction was implemented to render useful a 1 mA proton beam at 30 MeV to treat patients in the next generation of BNCT facilities [14,15].

In Argentina a project to develop a Tandem-ElectroStatic Quadrupole (TESQ) accelerator for accelerator-based BNCT is under way at the National Atomic Energy Commission. The machine is intended to be able to deliver a high intensity proton beam of approximately 30 mA at 2.3–2.4 MeV, based on the $^{7}$Li(p,n)$^{7}$Be reaction. Important progress was achieved in a number of different areas such as hardware associated to the facility, electrostatic field assessment, beam transport, tubes, beam shaping assembly (BSA), patient treatment room, computational dosimetry and treatment planning [16–23]. Regarding the latter, a theoretical study based on Monte Carlo simulations was performed to assess the treatment planning capability of different configurations of an optimized beam shaping assembly for such accelerator, which is a new way to test a BSA from a clinical point of view [24].

In this context, the goal of the present work is to explore the prospects for a potential use of the TESQ accelerator-based facility in the treatment of different tumor targets that are candidates for BNCT. The performance of the proposed BSA design associated to the facility has been theoretically analyzed using computed tomography (CT) data of patients through treatment planning and MCNP simulations. Tumors within the central nervous system and the head-and-neck region were considered. For these targets no clinical data for reactor-based BNCT treatments was available in our group and hence a set of real cases of patients who underwent standard radiotherapy containing some representative tumor positions and sizes was used in the present study. In addition, a set of clinical cases of malignant nodular melanoma treated with the B1 beam of the RA-6 nuclear reactor was used to make thorough comparisons with the accelerator-derived results. This last comparison allowed to evaluate the potential capabilities of the accelerator for real clinical scenarios under similar conditions and within the same protocol.

A feasibility study of a radiation therapy treatment should include not only the assessment of the effectiveness and radiotoxic effects in tissues but also the evaluation of the out-of-field dose delivered during treatment by normal organs distant from the irradiated target. In the present work a whole-body dose assessment using an analytical whole-body phantom was also included for the cases of interest.

## Materials and methods

The main purpose of the CNEA accelerator facility is to provide a machine that can be installed in hospitals and suitable to treat deep-seated tumor targets. Thus, our BSA design has been optimized [20,21,23] to produce the epithermal neutron beam required to treat these kind of tumors. In this procedure IAEA recommendations on beam quality were taken into account in order to achieve a similar performance as those of reactors. In addition, the present work shows that, from a clinical point of view, the designed BSA can also be applied to other targets when suitable treatment planning strategies are implemented.

Up to date intense research has been carried out on trials on central nervous system tumors, head-and-neck tumors and melanoma tumors using reactor-based BNCT [2,25–36]. For this reason, an extensive set based of this kind of targets was studied here considering clinical-like cases that cover both superficial and deep tumors of different sizes and locations. Each tumor location was analyzed according to the same protocol established by clinical institutions in Japan (Tsukuba), Finland and Argentina that have treated patients. In this manner we are able to compare our results with reported data and evaluate the potential effectiveness and radiotoxic effects of the accelerator-based therapy.

### *Beam shaping assembly design: spectrum and beam quality parameters*

Beam quality is strongly dependent on neutron fluxes and dose components which are identified as boron dose ($D_B$), thermal and fast neutron doses ($D_{th}$ and $D_f$, respectively) and gamma dose ($D_\gamma$). The first component stems from the interaction of thermal neutrons with $^{10}$B atoms in tissue through the $^{10}$B(n,$\alpha$)$^{7}$Li reaction meanwhile the second component arises primarily from the $^{14}$N(n,p)$^{14}$C thermal neutron capture reaction. Fast neutrons with energies above 10 keV deliver the third component (fast neutron dose) through elastic collisions with hydrogen nuclei in tissue via the $^{1}$H(n,n′)$^{1}$H reaction. Finally, the last component is related to photons that can be generated both in the device structure and through the $^{1}$H(n,$\gamma$)$^{2}$H reaction in tissue. Since four dose components contribute to the total absorbed dose, BNCT is said to use a mixed field of radiation. The weighted total dose $D$ is calculated as

$$D = w_B D_B + w_{th} D_{th} + w_f D_f + D_\gamma, \quad (1)$$

where $w_i$ is the radiobiologic weighting factor of dose component $D$ in a particular tissue and a given endpoint, which is used to express $D$ in photon-equivalent units (Gy). In this work all the expressed doses are radiobiological weighted unless otherwise indicated.

To provide the optimum clinical neutron beam with low incident gamma and fast neutron contaminations, an optimized beam shaping assembly was developed in our group for the accelerator-based facility assuming a 30 mA proton beam current at 2.3 MeV [37]. Briefly, the BSA (Fig. 1) consists in of cylindrical tube-like container of moderating materials and enriched $^{6}$Li lithium carbonate to filter the thermal neutrons. The moderator is formed by successive layers of aluminum, PTFE and lithium carbonate surrounded by a lead reflector that contributes to redirect the neutrons and shield the photons. Both the moderator and reflector form a solid cone shaped collimator with a 12 cm diameter output port. This collimator allows the proper patient positioning and as shielding from the undesired photons and fast neutrons that always exist in the mixed field of radiation. The circular neutron beam aperture of 12 cm diameter is shown in Fig. 1 together with the water cooling system of the target and the position of the metallic lithium target where the neutron source description is located for Monte Carlo simulations. The neutron production by the $^{7}$Li(p,n)$^{7}$Be reaction in the Li target is calculated according to the procedure described in Ref. [21].

According to IAEA recommendations [38], absorbed dose rate due to gamma rays per epithermal neutron flux ($\dot{D}_\gamma/\phi_{epi}$) and the absorbed dose rate due to fast neutrons per epithermal neutron flux ($\dot{D}_f/\phi_{epi}$) in existing BNCT facilities should be less than $2 \times 10^{-13}$ Gy cm$^2$ n$^{-1}$. Beam port parameters associated to the beam shaping assembly can be estimated using the general purpose Monte Carlo radiation transport code MCNP5 [39]. For this evaluation, the common definition for an epithermal energy range of 0.5 eV–10 keV was used and the average values were calculated

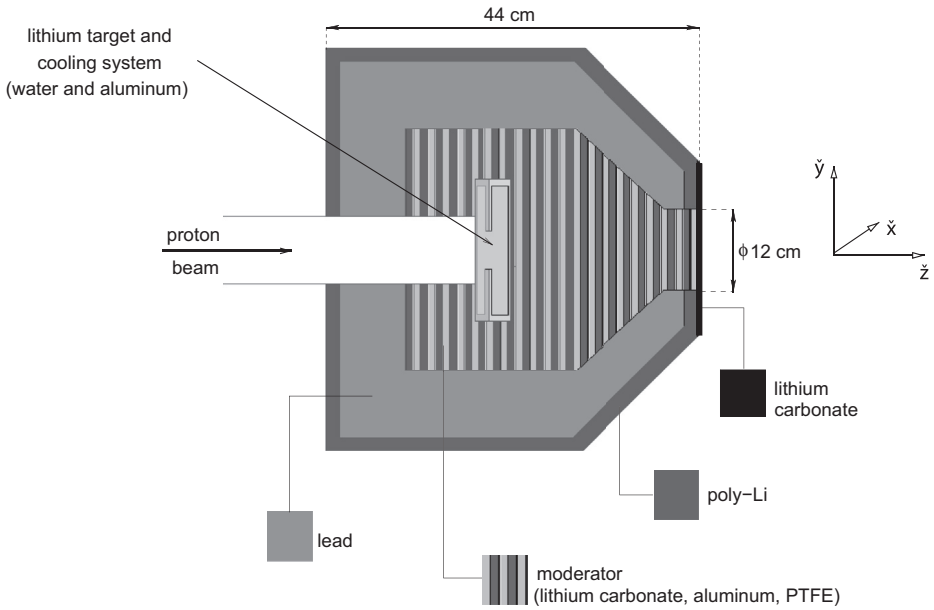


**Figure 1.** Schematic layout of the beam shaping assembly associated to the accelerator-based facility. Beam axis is indicated as ž.

across the beam aperture of the BSA. These two beam quality parameters derived from our BSA design are higher than IAEA's recommendations, but they are in the same range of those of some clinical reactor-based facilities (See Table 1). The non-compliance with these values does not rule out the possibility of very satisfactory performance, as will be shown in Results Section.

The neutron spectrum in-air at the exit port of the moderator is shown in Fig. 2. In our simulations the BSA proposed provides an incident epithermal neutron flux of 0.95 $\times$ $10^9$ n cm$^{-2}$ s$^{-1}$ with a thermal-to-epithermal neutron flux ratio of 0.008 and current to flux ratio ($J/\phi$) of about 0.7, in line approximately with those suggested by IAEA ($>10^9$ epithermal neutrons cm$^{-2}$ s$^{-1}$, $<$0.05 and $>$0.7, respectively). Therefore, the BSA scheme is promising in terms of beam quality and spectrum. In addition, other parameters will be evaluated from a clinical point of view to assess the accelerator-based facility in clinical-like cases.

*Protocols*

In the present section we will describe the clinical protocols used in this work that were established by different medical institutions in the treatment of brain tumors, head-and-neck tumors and malignant cutaneous melanoma with BNCT.

In 2005 the University of Tsukuba (Japan) established and approved a protocol to treat newly diagnosed glioblastoma multiforme (GBM) at the neutron beam facility installed in the Japan Research Reactor, JRR-4. The protocol combined fractionated photon therapy and a single BNCT irradiation using two boron delivery agents available for clinical BNCT trials, sulfhydryl borane (BSH) and *p*-dihydroxyboryl-phenylalanine (BPA) [30,47]. Patients were treated using this protocol until the phase I/II clinical trial was closed in 2007, while improvements to the reactor core were carried out.

For head-and-neck (H&N) tumors the protocol developed for the treatment of inoperable, recurrent, locally advanced head-and-neck cancer in Finland was considered. In this BPA-based BNCT trial, neutron irradiations were performed at the Finnish FiR-1 Triga Mark II nuclear research reactor. Each patient was scheduled to be treated twice at an interval of a few weeks [6]. The final analysis of the phase I/II trial based on 30 patients was recently published [32].

A phase I/II clinical trial for treating nodular melanoma (NM) with reactor-based BNCT was started in Argentina in 2003. From that date to 2007, when Argentina began the process of reconverting reactor cores to operate with low enriched uranium, seven patients were treated with the mixed neutron beam B1 of the RA-6 reactor (thermal neutron flux peak at about $10^9$ cm$^{-2}$ s$^{-1}$) accomplishing a total of ten irradiations. The developed Argentinian protocol uses BPA as boron delivery agent followed by a single neutron irradiation [35]. New licenses were recently obtained from the Argentine Nuclear Regulatory Authority to restart the clinical trial. The treatment protocols mentioned above are summarized in Tables 2 and 3. For dose calculations tissue-to-blood boron concentration ratios used in each trial were also considered assuming the mean of the average values computed during the treatments for

**Table 1**
In-air beam quality parameters derived from the accelerator-based facility and some examples of measured in-air parameters from epithermal reactor-based facilities. Power reactor and the beam diameter aperture for each facility are also shown. Other performance parameters are reported in the text. The bold font intents to give a relevance to the accelerator values, since the study of the accelerator is the aim of the present paper.

| Neutron source | $\phi_{epi}$ [$10^9$ n cm$^{-2}$ s$^{-1}$] | $\dot{D}_f/\phi_{epi}$ [$10^{-13}$ Gy cm$^2$ n$^{-1}$] | $\dot{D}_\gamma/\phi_{epi}$ [$10^{-13}$ Gy cm$^2$ n$^{-1}$] |
|---|---|---|---|
| **Accelerator (12 cm)** | **0.95** | **5.2** | **4.9** |
| FCB w/o filter (5 MW, 12 cm) [40] | 4.3 | 1.4 | 3.6 |
| JRR-4 (3.5 MW, 10–12 cm) [28] | 2.2 | 3.1 | 1.5 |
| THOR (1.2 MW, 14 cm) [41,42] | 1.1 | 3.4 | 1.3 |
| FiR-1 (0.25 MW, 14 cm) [43,44] | 1.1 | 2.1 | 0.5 |
| KURR (5 MW, 12 cm) [45] | 0.46 | 6.2 | 2.8 |
| HFR (45 MW, 12 cm) [46] | 0.33 | 12.1 | 3.8 |

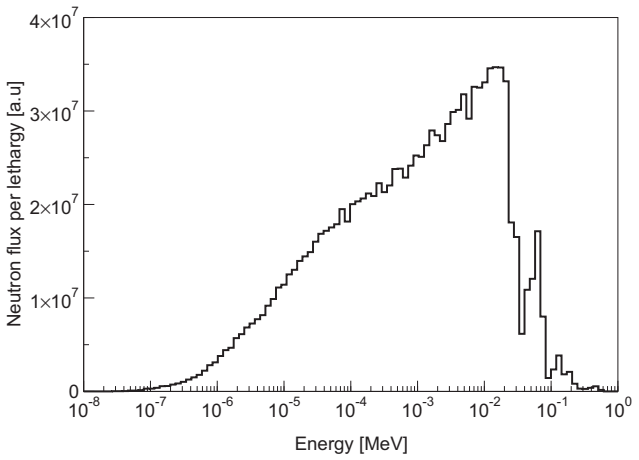


**Figure 2.** In-air neutron beam spectrum at the exit port.

the measured $^{10}$B concentration in blood in the GBM and H&N trials and in particular for NM the value was subjected to the retrospective data for each patient (Table 4).

*Clinical cases*

In the present section the clinical cases that were selected to cover the study of brain tumors (glioblastoma multiforme), head-and-neck tumors and cutaneous melanoma tumors (nodular melanoma) are presented. This set of cases included superficial and deep tumors of different sizes and locations (Table 5). Cases GBM #1 and #2 involved single lesions in the brain while case GBM #3 had multifocal tumors. For H&N cases #1 and #2, a transitional cell carcinoma in the left maxillary sinus and a squamous cell carcinoma tumor in the left lateral neck were considered. In particular, two patients that were irradiated in the RA-6 nuclear research reactor were selected as the clinical-like melanoma cases. Significant differences in the number of nodules and locations between patients are shown in Fig. 3. As can be observed NM #1 had two nodules in the right thigh while NM #2 had multiple subcutaneous skin metastases (10 nodules in total) on the external face of the right leg.

*Treatment planning and assessment*

Clinical target volumes (CTV) were defined as the gross tumor volume with an additional 1 cm margin in all directions for the GBM and H&N cases. For the NM cases a planning target volume with multiple melanomas was defined by the radiation oncologist for each case. Regions of interest including normal organs, were contoured in the patient's CT. Medical images were also used to create the three-dimensional Monte Carlo model of the geometry to be treated by partition the CT stack in 11,025 cubes or voxels of 1 cm$^3$, each one with a tissue composition weighted by the volume fraction of each material present in the cube [49]. For the MCNP simulations elemental tissue compositions were extracted from ICRU 46 [50]. In particular for case NM #2, approximately 2.5 cm of tissue equivalent bolus was needed to thermalize the neutron beam. For this purpose the CT images of the patient were modified using an image processing program, creating the tissue compensator of 2.5 cm thickness on the leg. The new stack, including both the leg and the bolus material was voxelized using the NCTPlan system [51].

An upgraded version of the NCTPlan v1.3 treatment planning code allowed us to prepare the input deck for the MCNP5 code using not only a particle planar source description but also the complete three-dimensional geometry of the BSA. In addition to both patient and BSA geometry and material descriptions, dose-to-kerma conversion factors for neutrons and photons reported in Ref. [52] were also included in the input. Typical MCNP runs involved $10^9$ particles yielding relative statistical errors of about 1% for each dose component computed in a voxel.

Single-field or multiple non-coplanar irradiation fields were selected (Table 5) in the treatment plans to maximize the dose delivered to tumors within the limits to normal tissues. In particular, single anterior–posterior fields were used in the H&N and NM tumors while for GMB tumors two- or three-field treatment plans were proposed to ensure a minimum tumor dose of 30 Gy for each GBM case analyzed. This value was derived by Laramore [53] as the minimum tumor dose capable of controlling a malignant glioma. Total equivalent dose distributions were calculated considering the $^{10}$B concentrations in normal tissue and tumor and the biological effectiveness factors described in detail for each protocol in Protocols Section. Where more than one field was simulated, equal

**Table 2**
Treatment protocols considered in this work for the different BNCT tumor targets.

| Protocols | GBM Tsukuba [47] | H&N Finland [32] | NM Argentina |
|---|---|---|---|
| Boron drug | BPA + BSH | BPA | BPA |
| Facility & beam | JRR-4 epithermal/mixed $\phi$ = 10, 12 cm | FiR-1 epithermal $\phi$ = 11, 14 cm | RA-6 mixed $\phi$ = 15 cm |
| Prescription peak dose | Brain 13 Gy | Mucosa 6 Gy[a] | Skin[b] 16.5–24.0 Gy[c] |
| RBE/CBE | Table 3 (col. I) | Table 3 (col. II) | Table 3 (col. III) |

[a] Absorbed dose (not weighted).
[b] Considered as a 5 mm-thick layer.
[c] Range of maximum skin doses delivered to the NM patients.

**Table 3**
Relative biological effectiveness (RBE) factors and compound biological effectiveness (CBE) factors used in each protocol.

| Protocols | Boron drug | RBE/CBE | | |
|---|---|---|---|---|
| | | GBM Tsukuba [48] | H&N Finland [6,26] | NM Argentina |
| Boron | BPA | 3.80 (tumor)<br>1.35 (brain)<br>2.50 (skin) | 3.8 (tumor)<br>1.3 (brain)<br>2.5 (mucosa) | 3.8 (tumor)<br>2.5 (skin) |
| | BSH | 2.50 (tumor)<br>0.37 (brain)<br>0.80 (skin) | | |
| Fast neutron | BPA | 2.5 | 3.2 | 3.0 |
| Thermal neutron | | 2.5 | 3.2 | 3.0 |
| Photon | | 1.0 | 1.0 | 1.0 |

**Table 4**
Mean blood-boron concentration and tissue-to-blood ratios from BNCT treatment data.

| Protocols | Boron drug | GBM | H&N | NM |
|---|---|---|---|---|
| | | Tsukuba | Finland | Argentina |
| Blood $^{10}$B concentration | BPA | 17.4 ppm[a] | 19.6 ppm[a] | 14.7/16.3 ppm[b] |
| | BSH | 34.6 ppm[a] | | |
| Tissue-to-blood ratio | BPA | 3.5 (tumor)<br>1.0 (brain)<br>1.5 (skin) | 3.5 (tumor)<br>1.0 (brain)<br>2.0 (mucosa) | 3.5 (tumor)<br>1.5 (skin) |
| | BSH | 1.0 (all tissues) | | |

[a] Mean of the average values computed during the treatments for the measured $^{10}$B concentration in blood [6,47].
[b] Values selected from the real data of the two NM patients considered in this paper.

**Table 5**
Tumor sizes and locations for the different targets. The number of beams used in the treatment planning and their orientation are also shown.

| Case ID | | Tumor | | | |
|---|---|---|---|---|---|
| | | Volume [$cm^3$] | Depth[a] [cm] | Location | No of fields & orientation[b] |
| GBM | #1 | 18.5 | 3.9 | Occipital lobe | 2 RPO LPO |
| | #2 | 6.4 | 6.5 | Temporo–occipital lobe | 3 SPO RPO LPO |
| | #3 | 25.9 | 4.0 | Frontal lobe | 3 LSL LL P |
| | | 2.2 | 3.4 | Temporal lobe | |
| | | 4.2 | 3.5 | Occipital lobe | |
| H&N | #1 | 12.9 | 2.2 | Maxillary sinus | 1 AP |
| | #2 | 120.0 | 7.2 | Lateral neck | 1 AP |
| NM | #1 | 0.35/0.45 | ~1 | Thigh | 1 AP |
| | #2 | 0.09–0.87 | Superficial | Leg | 1 AP |

[a] Defined as the minimum distance between the skin and the center of mass of the tumor.
[b] RPO: right posterior oblique, LPO: left posterior oblique, SPO: superior posterior oblique, LSL: left superior lateral, LL: left lateral, P: posterior, AP: anterior posterior.

mean blood-boron concentration was assumed for each field (i.e. the boron concentration remained the same for each irradiation).

Since the results obtained from the RA-6 reactor were available for us, they could be thoroughly compared with the accelerator-based simulations. For this purpose, all parameters associated with the irradiation of cases NM #1 and #2 remained the same, including the boron concentration, prescription dose and field orientation. At the time of the irradiations, physical characteristics of the treatment room in the BNCT facility imposed limit on the positioning of the patient. Thus, in order to determine the maximum performance achievable by the accelerator in such treatments, a second treatment planning was performed for each melanoma case. An improved or optimized beam direction (OBD) was selected according to the potential benefits that would be provided by the larger treatment room and the presence of the external collimator.

According to the characteristics of the particular case analyzed, a set of different figures of merit (FOMs) was selected to assess the dosimetry performance of the treatment. As clinical-like cases of both GBM and H&N involved the irradiation of normal organs in the head, the same figures of merit including the treatment time, tumor and normal tissue dosimetry and cumulative dose-volume histograms (DVHs) were employed.

Due to the fact that the principal organ at risk in an NM treatment is the normal skin, other figures were added to the already mentioned set of FOMs. In particular, since early toxicity is related to the irradiation delivered to the epidermis and subpapillary dermis, the superficial dose distribution for normal skin was evaluated through the cumulative dose-area histogram (DAH) instead

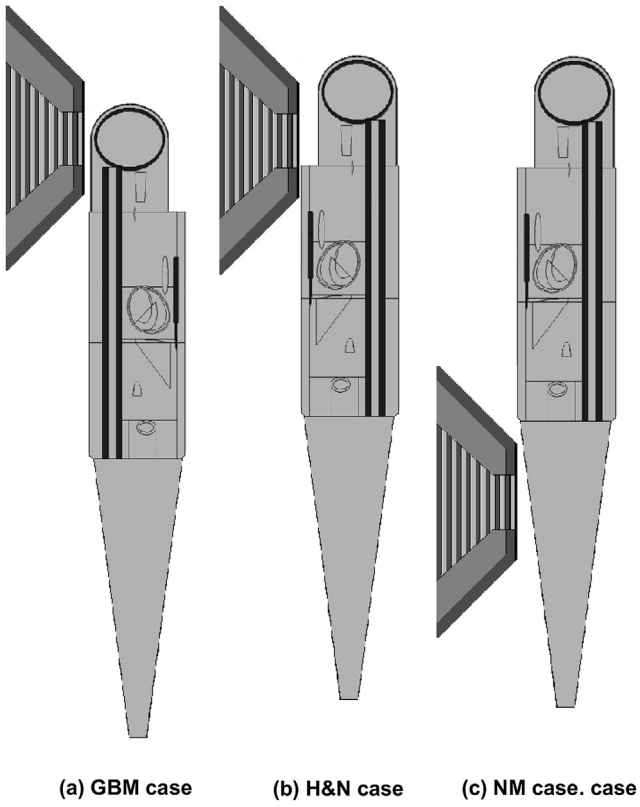


**Figure 4.** Schematic view of the beam direction selected to evaluate the whole-body dose to the patient through the MIT MIRD whole-body phantom, for each tumor target analyzed.

of DVH. A normal tissue complication probability model (NTCP) based on the inhomogeneous dose distributions at the most superficial layer of the skin, as proposed by González et al. was also used to take into account possible early skin effects [54]. Moreover, the maximum dose to the skin, the mean dose in the 100 $cm^2$ of skin that received the highest doses and the related probability-equivalent uniform dose to the skin were included in the evaluation of the melanoma cases.

The out-of-field dose delivered in the treatment to normal organs was also included as a FOM. For this purpose the analytical whole-body MIT MIRD phantom distributed by Los Alamos was used. The phantom was positioned in the most unfavorable field according to each beam direction simulated in the clinical-like cases (i.e. three simulations were performed, one for each target).

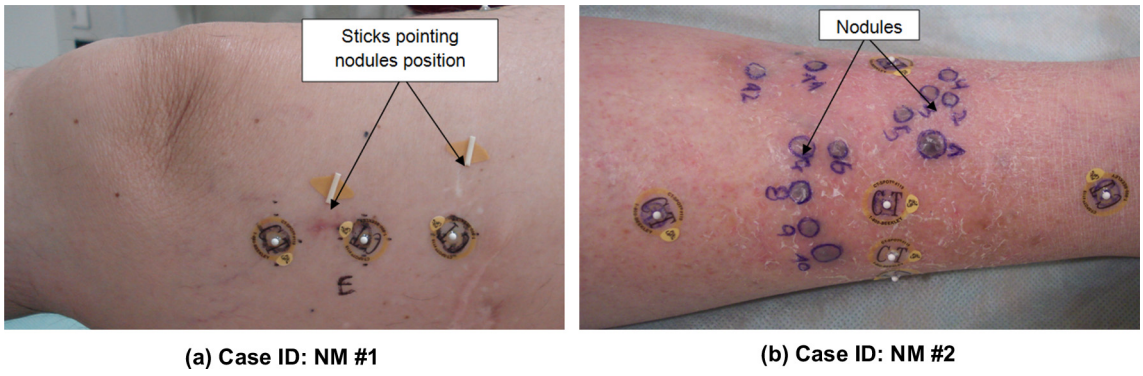


**Figure 3.** Patient photographs showing the lesions (a) pointed out by sticks and (b) at the superficial level of the skin.

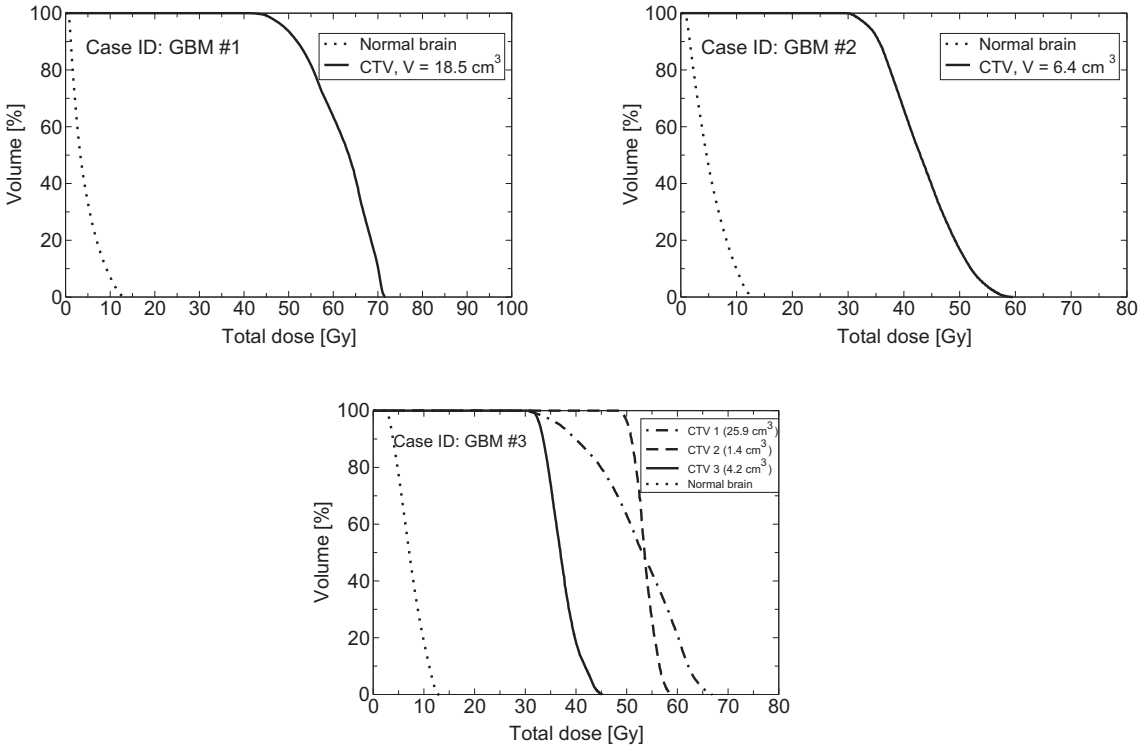


**Figure 5.** Cumulative dose-volume histograms for normal brain (both hemispheres) and the clinical target volumes (CTV) evaluated in the brain tumor cases GBM #1 (two-fields), #2 (two-fields) and #3 (three-fields).

Taking into account the three simulations, a total of ten organs (brain, pharynx, thyroid, thymus, lungs, liver, spleen, stomach, pancreas and testes) were evaluated. The mean absorbed dose rate in the mentioned organs was computed according to the available CBE and RBE values for liver and lung [55,56]. For other organs, the factors used for brain were assumed (See Table 3, col. II). The tissue-to-blood boron concentration ratio of 1:1 was used for all organs. In Fig. 4 the schematic view of the beam direction selected to evaluate the whole-body dose to the patient in the MIT MIRD phantom is shown for each case.

## Results

### *Glioblastoma multiforme*

Subject to the maximum dose to normal brain of 13 Gy used in the brain tumor protocol described in detail in Protocols Section, cases GBM #1, #2 and #3 resulted in similar irradiation times of about 20 min for each field. Since two- or three-field arrangements were used in the simulations, a complete treatment irradiation time would be achievable in 1 h. Due to the fact that multiple fields were used, significant attention should be given to the dose delivered to the normal brain. Simulations gave an average whole-brain dose of 4.2, 5.2 and 7.0 Gy respectively. In the cumulative dose-volume histograms of Fig. 5 for normal brain the expected increase in the mean dose can be seen with the increase in the number of radiation fields. Other normal organs in the head such as eyes, optic nerves and chiasm received a maximum dose lower than 2.8 Gy and a mean dose lower than 1.5 Gy. The DVHs also show the dose delivered to each CTV. According to the strategy used in the treatment plans, 100% of the tumor received more than 30 Gy, reaching minimum doses of 40 or almost 50 Gy, subject to the size of the tumor and its location in the brain.

The clinical outcome of eight patients with newly diagnosed, histologically confirmed GBM and with no prior conventional radiotherapy or chemotherapy was published by Yamamoto et al.

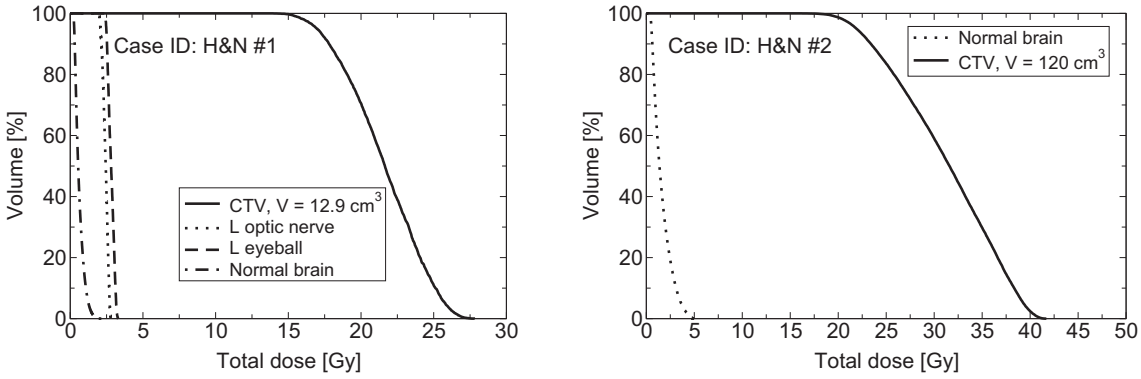


**Figure 6.** Cumulative dose-volume histograms for the clinical target volume (CTV) and normal brain (both hemispheres) for the H&N cases (single-field).

**Table 6**
Mean (minimum – maximum) tumor doses derived from the accelerator simulations using the reactor and an optimized beam direction (RBD and OBD, respectively). The retrospective tumor doses from the RA-6 reactor are also shown.

| Source | Total dose [Gy] | |
|---|---|---|
| | Nodule 1 | Nodule 2 |
| RA-6 reactor | 38.9 (37.4–40.8) | 30.0 (25.7–33.1) |
| Accelerator (RBD) | 49.1 (38.0–56.4) | 39.5 (34.7–44.7) |
| Accelerator (OBD) | 50.4 (38.7–56.5) | 50.3 (44.0–55.0) |

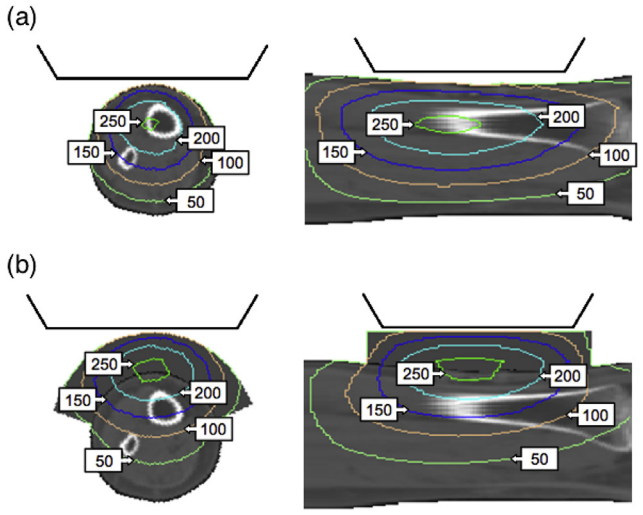


**Figure 7.** (Color online) Tumor isodose curves for NM #2 under the optimized beam direction without a bolus material (a) and with a bolus implementation (b). Curves are normalized to the maximum dose of 22.6 Gy at the skin and are expressed as a percentage of that maximum. Note that the last condition provided a usable neutron energy range in the treatment of superficial nodules.

[30]. These patients were treated according to the previously described protocol in Protocols Section. The reported averaged values of the minimum tumor dose delivered to the CTV were 29.8 ± 9.9 Gy and a mean brain dose of 3.9 ± 0.4 Gy. The most common acute adverse effect observed in the group was erythema (grade 1) and no damage associated with the brain irradiation was observed. Based on these results the authors have derived 1- and 2-year survival rates of 80 and 53.3%, respectively. In our simulations we could deliver to the CTVs at least 30 Gy in all cases with average whole-brain doses between 4.2 and 7.0 Gy. In the Japanese experience, a mean brain dose of 6.2 Gy was associated to 50% of somnolence occurrence [30]. This is also consistent with previous findings from the Brookhaven and Harvard-MIT patient data set [57,58] that indicated that such toxicity was obtained for average brain doses between 5 and 7 Gy. The average doses found in our results for cases GBM #2 and #3 are in the range of those delivered in the mentioned clinical trials. Thus, the same radiotoxicity effects as reported in Refs. [30,57,58] for normal brain should be expected.

*Head-and-neck*

Subject to the mucosal membrane absorbed dose constraint of 6 Gy (not weighed), the irradiation times for the head-and-neck cases, H&N #1 and #2, were 24 and 36 min. The normal organs in the head such as brain, eyes, and chiasm received mean doses lower than 2 Gy. The organ that received the highest dose because of its location close to the target, was the larynx with a maximum mean dose of 4.7 Gy. This value is lower than the maximum acceptable dose of 10 Gy adopted in the Finnish protocol for all organs except the mucosa. As can be deduced from the cumulative DVHs plotted in Fig. 6, the minimum doses delivered to the CTVs for cases #1 and #2 were 14 and 16 Gy (with mean doses of 21 and 31 Gy, respectively). Taking into account that our study is subjected to the Finnish protocol, these values agree with those achieved in their clinical applications. A mean average tumor dose of 22 Gy with a range of 15–33 Gy and 21 Gy between 15 and 28 Gy was reported by L. Kankaanranta et al. for the first and second BNCT irradiations. Based on the mentioned procedure performed at the FiR-1 nuclear research rector in Finland, 76% of the patients achieved a complete or partial response to BNCT, while 27% of them survived for 2-years without loco-regional recurrence [6,32].

*Nodular melanoma*

As stated in the Treatment planning and assessment Section of cases NM #1 and #2, the reactor beam direction (RBD) and the optimized beam direction (OBD) were used to study the dosimetry derived from the BSA. Both plans will be analyzed in each case considering the different figures of merit related to treatment time, tumor dosimetry and possible skin damage. Subject to the maximum dose administered to the skin in the real treatments (20.8 and 22.6 Gy for cases #1 and #2, respectively), irradiation times derived from simulations were close to 1 h for both reactor and optimized field orientations. In particular, for case NM #1 times

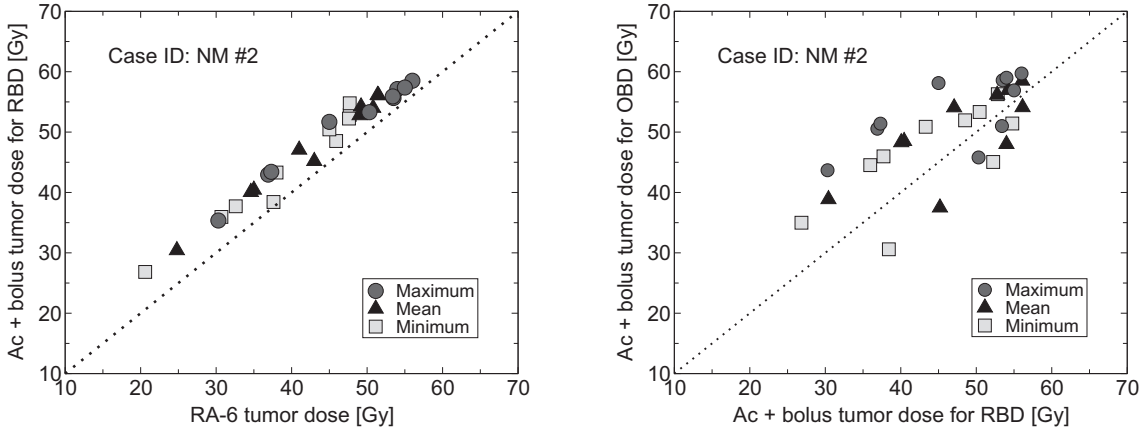


**Figure 8.** Maximum, mean and minimum doses delivered to the 10 nodules involved in case NM #2 for: (left) RA-6 reactor-based results vs. accelerator-based results with bolus and the reactor beam direction (RBD) and (right) accelerator-based results with bolus and the optimized beam direction (OBD) vs. the same for the RBD.

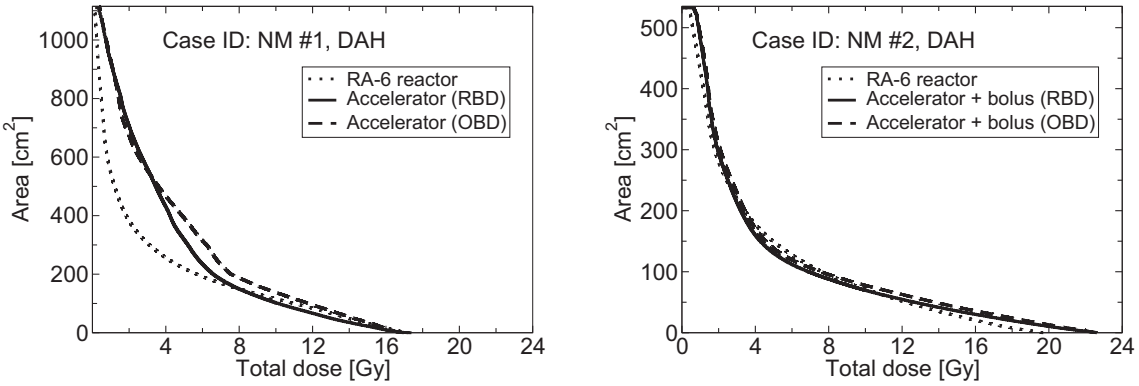


**Figure 9.** Cumulative dose-area histograms for the skin derived from the accelerator simulations considering the reactor beam direction (RBD) and the optimized beam direction (OBD). The derived DAH from the real irradiation with the RA-6 reactor is also shown.

of 56 and 53 min for RBD and OBD respectively, show no difference compared to the real irradiation time of 56 min. On the other hand, for case #2 the irradiation time of 43 and 44 min for RBD and OBD, respectively, was below the real treatment time of 75 min. Hence all the accelerator simulations gave acceptable irradiation times, equal to or less than those used in the real melanoma treatments. Regarding tumor doses, in the Table 6 accelerator-based tumor dosimetry for case NM #1 is presented together with the results obtained from the retrospective clinical analysis. As can be seen, physical limits on positioning of the patient in the real treatment lead to a low dose to nodule 2 compared with that of nodule 1. When RBD is used in the accelerator simulation, the difference in the minimum dose between nodules is reduced, showing that even maintaining the reactor field orientation the doses would be improved with the proposed accelerator-based neutron source. Also the maximum and mean doses delivered to the nodules are higher than those achieved with the reactor with identical field orientation and protocol, showing the potential applicability of the proposed BSA in a treatment like this. Moreover, the minimum, mean and maximum tumor doses could be enhanced if the OBD was used. In particular when the OBD is compared to the RBD an improvement in the minimum and mean dose of about 30% is achieved for nodule 2.

A tumor response analysis based on the clinical outcome of the patients treated in Argentina [54] reveals that for tumor volumes larger than 0.1 cm$^3$, minimum and mean doses up to 40 Gy produce a moderate tumor control (40 and 30%, respectively). Given these findings and taking into account that the tumor volumes analyzed in the present case are larger than 0.3 cm$^3$, the minimum doses of approximately 40 and 50 Gy achieved in nodules 1 and 2, and the mean dose greater than 50 Gy for both nodules could increase the likelihood of tumor control, providing a potential clinical benefit under the OBD planning.

Since case NM #2 involved superficial nodules, the bolus implementation was needed to provide a usable neutron energy range. As can be seen in Fig. 7, the introduction of 2.5 cm of tissue compensator material on the leg could provide the correct shift of the tumor isodose curves, leading to curves between 250 and 150% (normalized to the maximum peak skin dose of 22.6 Gy) in the tumor region. The minimum, mean and maximum doses derived from the accelerator irradiation are compared with those achieved in the real irradiation in Fig. 8 subject to the reactor field orientation. In the same figure, a second comparison is also shown between both simulated beams to determine the attainable performance of the BSA. As can be seen in the figure, the accelerator with bolus would provide a treatment at least equal to the one performed in the RA-6 from a tumor dosimetry point of view if RBD was used. Furthermore, when the OBD is used eight of the ten nodules received minimum tumor doses higher than 35 Gy. Also subject to this field orientation, the mean doses delivered to all nodules are higher than 40 Gy, thus providing a potential clinical benefit.

In summary, all treatment plans studied for cases NM #1 and NM #2 led to acceptable tumor doses compared with the results derived from the clinical irradiations, showing the potential use of the accelerator in the treatments of nodular melanomas. Assessment of the normal tissue dosimetry will now be presented considering the potential damage to the skin, the principal organ at risk. Since early toxicity is related to the irradiation delivered to the epidermis and subpapillary dermis, the superficial dose distribution for normal skin is evaluated through the cumulative dose-area histograms shown in Fig. 9. For single-fraction photon irradiations,

**Table 7**
Normal tissue complication probability (NTCP) computed for the accelerator treatment plans and reactor irradiations.

| Case ID | Source & beam direction | NTCP [%] |
|---|---|---|
| NM #1 | RA-6 reactor | 73 |
| | Accelerator RBD | 64 |
| | Accelerator OBD | 74 |
| NM #2 | RA-6 reactor | 77 |
| | Accelerator + bolus RBD | 92 |
| | Accelerator + bolus OBD | 95 |

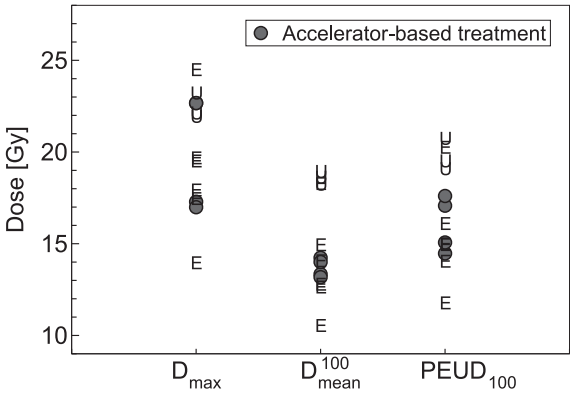


**Figure 10.** Figures of merit (FOMs) based on doses together with the assessed clinical outcome for all the irradiated patients in Argentina (E: erythema and U: ulceration). Filled circles are the corresponding values obtained with the accelerator-based beam for the two selected patients. The computed FOMs for the reactor beam direction and the optimized beam direction are shown.

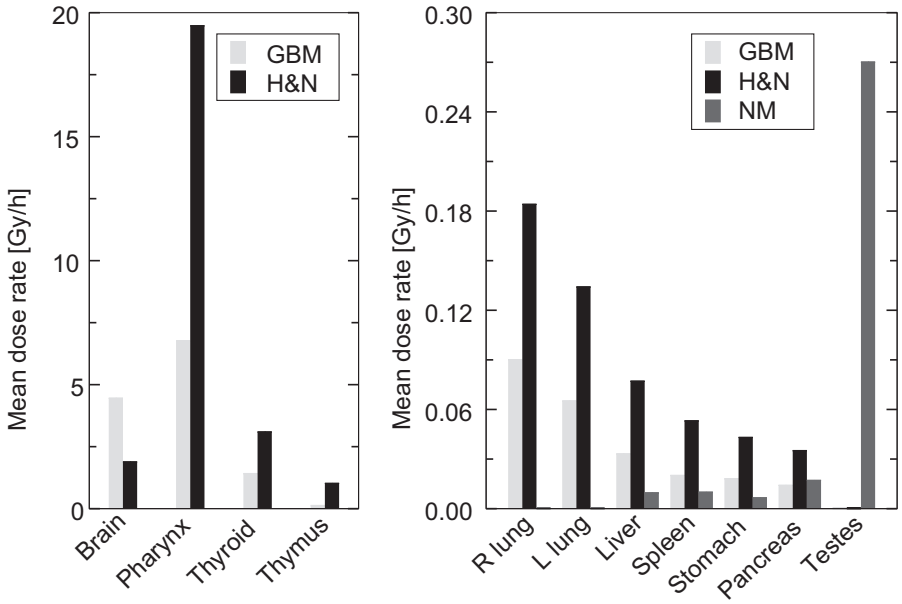


**Figure 11.** Mean weighted dose rate in normal organs for GBM, H&N and NM treatments. Dose rate in brain was also computed as a control data (which represent a mean brain dose of 5.1 and 0.7 Gy for GBM and H&N, respectively, in agreement with the reported doses in the corresponding cases, GBM #2 and H&N #1).

skin moist desquamation appears to be related to doses between 15 and 20 Gy in fields of about 100 $cm^2$ in size [59–61], thus no severe acute skin reaction would be expected if the proposed BSA was used in treatments of cases such as NM #1 and #2. Other figures of merit based on the dose distribution can be used to quantify possible acute skin damage. In particular, the normal tissue complication probability (NTCP) for inhomogeneous dose distributions was computed to take into account a radiobiological FOM. Based on the reported clinical data available to fit the parameters of the model, the figure determined the probability of developed dry desquamation. Due to the fact that the mentioned endpoint is fully accepted from a clinical point of view, we used the model to establish a relative comparison between the different sources and treatment plans. As can be seen in Table 7, the NTCP values obtained for case NM #1 for both RBD and OBD are consistent with those determined for the reactor. Higher probabilities were obtained for case #2, reaching 95%. As an estimation of other possible skin reactions, the assessed clinical outcomes of every patient that has been irradiated in the Argentinean melanoma clinical trial was used. The maximum dose to the skin ($D_{max}$), the mean dose in the 100 $cm^2$ of skin ($D^{100}_{mean}$) that received the highest doses and the related probability-equivalent uniform dose, $PEUD_{100}$, which is the uniform dose in 100 $cm^2$ of skin that gives the same NTCP as the actual inhomogeneous dose distribution, were computed for each accelerator-based treatment plan. The results shown in Fig. 10 are compared with those FOMs computed for all the irradiated patients that developed some skin reaction related with mild and severe toxicities, scored as erythema or ulceration. As can be seen in the figure, all of our results are placed in the region of an acceptable skin erythema for figures $D^{100}_{mean}$ and $PEUD_{100}$ defined quantities, while for $D_{max}$ only one treatment plan is obtained in a region with ulceration and erythema, showing that the accelerator can be used in this kind of treatment.

*Whole-body dose assessment*

As mentioned earlier, the clinical dose assessment should include the dose delivered to normal organs that are outside the treatment field. As can be observed in Fig. 11, two dose rate data sets are distinguishable related to the proximity between the studied organ and the neutron beam. As expected, organs near the head-and-neck region have the highest values for the GBM and H&N treatments while for the NM treatment the testes have the highest dose rate because of their proximity to the thigh. Here it is important to note, that while the brain is not considered an organ that is outside the treatment field, it was nevertheless included in the evaluation as a control in the first two treatments. The computed mean dose rate values of 4.45 and 1.88 Gy $h^{-1}$ in the GBM and H&N simulations, respectively, resulted in agreement with the obtained photon-equivalent doses of 5.2 and 0.7 Gy for cases GBM #2 and H&N #1, respectively, assuming identical treatment times, RBE and CBE factors and boron concentrations. On the other hand, the dose rate in the pharynx is quite high (19.5 Gy $h^{-1}$) for the H&N treatment, however if this value is converted to photon-equivalent units, it results in 7.8 Gy which is less than the maximum tolerable weighted dose admitted for all organs (this excludes the mucosal membrane) in the Finnish trial of 10 Gy. In a real treatment this dose may be reduced due to proper neck shielding. Other organs distant from the beam such as lungs, liver, spleen, stomach and pancreas have mean absorbed dose rates lower than 0.2 Gy $h^{-1}$. The main dose component is related to photons, reaching more than 95% of the total dose rate for those organs beyond the liver for GBM and H&N treatment and up to the pancreas for NM. In summary, all cases show low dose rate values for those organs very distant from the irradiated target and acceptable values for those which are nearest. Moreover, the maximum values that were converted to photon-equivalent doses are below the tolerable doses subject to the same protocols used in the present paper.

## Conclusions

Our results show that the proposed accelerator-BSA design is suitable for treating different targets, comprising superficial and deep-seated tumors. Following different established clinical protocols in BNCT for glioblastoma, head-and-neck tumors and

malignant cutaneous melanoma, and optimizing the treatment planning for each case analyzed, the proposed accelerator-BSA design yielded a tumor and normal tissue dosimetry and irradiation times as good as, if not better, that those reported for reactor-based BNCT.

## Acknowledgments

The authors wish to acknowledge financial support from CONICET and ANPCyT grant PICT-2010-2325, computed tomographies supplied by Amilcar Osorio from Fundación Centro Diagnóstico Nuclear and technical assistance from Rubén Farías.

## References

[1] Slatkin DN. A history of boron neutron capture therapy of brain tumors. Postulation of brain radiation dose tolerance limit. Brain 1991;114:1609–29.
[2] Wang LW, Wang SJ, Chu PY, Ho CY, Jiang SH, Liu YWH, et al. BNCT for locally recurrent head and neck cancer: preliminary clinical experience from a phase I/II trial at Tsing Hua open-pool reactor. Appl Radiat Isot 2011;69:1803–6.
[3] Fukutsuji K, Aihara T, Hiratsuka J, Kumada H, Ono K, Sakurai Y, et al. Boron neutron capture therapy for patients with melanomas of head-and-neck. In: Zonta A, editor. 13th International congress on neutron capture therapy, a new option against cancer 2008. p. 83–5. Florence, Italy.
[4] Suzuki M, Sakurai Y, Hagiwara S, Masunaga S, Kinashi Y, Nagata K, et al. First attempt of boron neutron capture therapy (BNCT) for hepatocellular carcinoma. Jpn J Clin Oncol 2007;37:376–81.
[5] Miyatake S, Tamura Y, Kawabata S, Lida K, Kuroiwa T, Ono K. Boron neutron capture therapy for malignant tumors related to meningiomas. Neurosurgery 2007;61:82–90.
[6] Kankaanranta L, Seppälä T, Koivunoro H, Saarilahti K, Atula T, Collan J, et al. Boron neutron capture therapy in the treatment of locally recurred head and neck cancer. Int J Radiat Oncol Biol Phys 2007;69:475–82.
[7] Howard W, Yanch J, Grimes S, Massey T, Al-Quraishi S, Jacobs D, et al. Measurements of the $^{9}$Be(p,n) thick target spectrum for use in accelerator-based BNCT. Med Phys 1996;23:1233–6.
[8] White SM. Beam characterization for accelerator-based BNCT using the $^{9}$Be(d,n) nuclear reaction. Ph.D. thesis. Massachusetts Institute of Technology: Cambridge; 1998.
[9] Burlon AA, Kreiner AJ, White S, Blackburn B, Gierga D, Yanch J. In-phantom dosimetry for the $^{13}$C(d,n)$^{14}$N reaction as a source for accelerator-based BNCT. Med Phys 2001;28:796–803.
[10] Harmon J, Kudchadker R, Kunze J, Serrano S, Zhou X, Harker Y, et al. Accelerator neutron sources for neutron capture therapy using near threshold charged particle reactions. In: Duggan J, Morgan I, editors. Application of accelerators in research and industry, proceedings of the fourteenth international conference. Denton, Texas: AIP Conf. Proc.; 1996. p. 123–6.
[11] Colonna N, Beaulieu L, Phair L, Wozniak G, Moretto L, Chu W, et al. Measurements of low-energy (d,n) reactions for BNCT. Med Phys 1999;26:793–8.
[12] Yoshioka M, Matsumura A, Kumada H, Sakurai Y, Kiyanagi Y, Hiraga F, et al. Development of an accelerator based BNCT facility in Ibaraki. In: 15th International congress on neutron capture therapy. Tsukuba, Japan; 2012.
[13] Kumada H, Matsumura A, Sakurai H, Sakae T, Yoshioka M, Kobayashi H, et al. Project of development of the linac based NCT facility in University of Tsukuba. In: 15th International congress on neutron capture therapy. Tsukuba, Japan; 2012.
[14] Tanaka H, Sakurai Y, Suzuki M, Masunaga S, Kinashi Y, Kashino G, et al. Characteristics comparison between a cyclotron-based neutron source and KUR-HWNIF for boron neutron capture therapy. Nucl Instrum Methods Phys Res B 2009;267:1970–7.
[15] Suzuki M, Tanaka H, Sakurai Y, Kashino G, Yong L, Masunaga S, et al. Impact of accelerator-based boron neutron capture therapy (AB-BNCT) on the treatment of multiple liver tumors and malignant pleural mesothelioma. Radiother Oncol 2009;92:89–95.
[16] Kreiner AJ, Castell W, Di Paolo H, Baldo M, Bergueiro J, Burlon AA, et al. Development of a tandem-electrostatic-quadrupole facility for accelerator-based boron neutron capture therapy. Appl Radiat Isot 2011;69:1672–5.
[17] Vento VT, Bergueiro J, Cartelli D, Valda AA, Kreiner AJ. Electrostatic design and beam transport for a folded tandem electrostatic quadrupole accelerator facility for accelerator-based boron neutron capture. Appl Radiat Isot 2011;69:1649–53.
[18] Cartelli D, Vento VT, Castell W, Di Paolo H, Kesque JM, Bergueiro J, et al. Accelerator tube construction and characterization for a tandem-electrostatic-quadrupole for accelerator-based boron neutron capture therapy. Appl Radiat Isot 2011;69:1680–3.
[19] Bergueiro J, Igarzabal M, Sandin JCS, Somacal HR, Vento VT, Huck H, et al. Development of high intensity ion sources for a tandem-electrostatic-quadrupole facility for accelerator-based boron neutron capture therapy. Appl Radiat Isot 2011;69:1676–9.
[20] Burlon AA, Girola S, Valda AA, Minsky DM, Kreiner AJ, Sánchez G. Design of a beam shaping assembly and preliminary modelling of a treatment room for accelerator-based BNCT. Appl Radiat Isot 2011;69:1688–91.
[21] Minsky DM, Kreiner AJ, Valda AA. AB-BNCT beam shaping assembly based on $^{7}$Li(p,n)$^{7}$Be reaction optimization. Appl Radiat Isot 2011;69:1668–71.
[22] Burlon AA, Kreiner AJ. A comparison between a TESQ accelerator and a reactor as neutron sources for BNCT. Nucl Instrum Methods Phys Res B 2008;266:763–71.
[23] Burlon AA, Kreiner AJ, Valda AA, Minsky DM, Somacal HR, Debray DE, et al. Optimization of a neutron production target and beam shaping assembly based on the $^{7}$Li(p,n)$^{7}$Be reaction. Nucl Instrum Methods Phys Res B 2005;229:144–56.
[24] Herrera MS, González SJ, Burlon AA, Minsky DM, Kreiner AJ. Treatment planning capability assessment of a beam shaping assembly for accelerator-based BNCT. Appl Radiat Isot 2011;69:1870–3.
[25] Diaz AZ. Assessment of the results from the phase I/II boron neutron capture therapy trials at the Brookhaven National Laboratory from a clinician point of view. J Neurooncol 2003;62:101–9.
[26] Joensuu H, Kankaanranta L, Seppälä T, Auterinen I, Kallio M, Kulvik M, et al. Boron neutron capture therapy of brain tumors: clinical trials at the Finnish facility using boronophenylalanine. J Neurooncol 2003;62:123–34.
[27] Kato I, Ono K, Sakurai Y, Ohmae M, Maruhashi A, Imahori Y, et al. Effectiveness of BNCT for recurrent head and neck malignancies. Appl Radiat Isot 2004;61:1069–73.
[28] Nakagawa Y, Pooh K, Kobayashi T, Kageji T, Uyama S, Matsumura A, et al. Clinical review of the Japanese experience with boron neutron capture therapy and a proposed strategy using epithermal neutron beams. J Neurooncol 2003;62:87–99.
[29] Miyatake S, Kawabata S, Yokoyama K, Kuroiwa T, Michiue H, Sakurai Y, et al. Survival benefit of boron neutron capture therapy for recurrent malignant gliomas. J Neurooncol 2009;91:199–206.
[30] Yamamoto T, Nakai K, Kageji T, Kumada H, Endo K, Matsuda M, et al. Boron neutron capture therapy for newly diagnosed glioblastoma. Radiother Oncol 2009;91:80–4.
[31] Fuwa N, Suzuki M, Sakurai Y, Nagata K, Kinashi Y, Masunaga S, et al. Treatment results of boron neutron capture therapy using intra-arterial administration of boron compounds for recurrent head and neck cancer. Br J Radiol 2008;81:749–52.
[32] Seppälä LKT, Koivunoro H, Saarilahti K, Atula T, Collan J, Salli E, et al. Boron neutron capture therapy in the treatment of locally recurred head-and-neck cancer: final analysis of a phase I/II trial. Int J Radiat Oncol Biol Phys 2012;82:e67–75.
[33] Fukuda H, Honda N, Wadabayashi N, Kobayashi T, Yoshino K, Hiratsuka J, et al. Pharmacokinetics of $^{10}$B-p-boronopheny-lalanine in tumors, skin and blood of melanoma patients: a study of boron neutron capture therapy for malignant melanoma. Melanoma Res 1999;9:75–83.
[34] Madoc-Jones H, Zamenhof R, Solares G, Harling O, Yam CS, Riley K, et al. A phase-I dose escalation trial of boron neutron capture therapy for subjects with metastatic subcutaneous melanoma of the extremities. In: Mishima Y, editor. Cancer neutron capture therapy. New York: Plenum Press; 1996. p. 707–16.
[35] González SJ, Bonomi MR, Santa Cruz GA, Blaumann HR, Larrieu OAC, Menéndez P, et al. First BNCT treatment of a skin melanoma in Argentina: dosimetric analysis and clinical outcome. Appl Radiat Isot 2004;61:1101–5.
[36] Menéndez PR, Roth BM, Pereira MD, Casal MR, González SJ, Feld DB, et al. BNCT for skin melanoma in extremities: updated Argentine clinical results. Appl Radiat Isot 2009;67:S50–3.
[37] Minsky DM, Kreiner AJ. Beam shaping assembly optimization for $^{7}$Li(p,n)$^{7}$Be reaction accelerator based BNCT. In: 15th International congress on neutron capture therapy. Tsukuba, Japan; 2012.
[38] Current status of neutron capture therapy. TECDOC-1223. Viena: IAEA; 2001.
[39] A general Monte Carlo N particle transport code. LA-UR-03-1987 version 5. LANL; 2003.
[40] Riley KJ, Binns PJ, Harling OK. Performance characteristics of the MIT fission converter based epithermal neutron beam. Phys Med Biol 2003;48:943–58.
[41] Liu Y-H, Nievaart S, Tsai P-E, Liu H-M, Moss R, Jiang S- H. Neutron spectra measurement and comparison of the HFR and THOR BNCT beams. Appl Radiat Isot 2004;67:S137–40.
[42] Tung CJ, Wang YL, Hsu FY, Chang SL, Liu YWH. Characteristics of the new THOR epithermal neutron beam for BNCT. Appl Radiat Isot 2004;61:861–4.
[43] Seppaälä T. FiR 1 epithermal neutron beam model and dose calculation for treatment planning in neutron capture therapy. Ph.D.Thesis. Report Series in Physics, HU-P-D103. University of Helsinki: Helsinki, Finland; 2002.
[44] Auterinen I, Hiismäki P, Kotiluoto P, Rosenberg RJ, Salmenhaara S, Seppaälä T, et al. Metamorphosis of a 35 years old Triga reactor into a modern BNCT facility. In: Hawthorne MF, Shelly K, Wiersema RJ, editors. Frontiers in neutron capture therapy. New York: Plenum Press; 2001. p. 267–75.
[45] Sakurai Y, Kobayashi T. The medical-irradiation characteristics for neutron capture therapy at the Heavy Water Neutron Irradiation Facility of Kyoto University Research Reactor. Med Phys 2002;29:2328–37.
[46] Binns PJ, Riley KJ, Harling OK. Dosimetric comparison of six epithermal neutron beams using an ellipsoidal water phantom. In: Sauerwein W, editor. Research and development in neutron capture therapy. Bologna, Italy: Monduzzi Editore; 2002. p. 405–9.
[47] Yamamoto T, Nakai K, Matsumura A. Boron neutron capture therapy for glioblastoma. Cancer Lett 2008;262:143–52.

[48] Kumada H. Personal communication 2011.
[49] González SJ, Carando DG, Santa Cruz GA, Zamenhof RG. Voxel model in BNCT treatment planning: performance analysis and improvements. Phys Med Biol 2005;50:441–58.
[50] ICRU Report 46D. Bethesda-Maryland, USAPhoton, electron, proton and neutron interaction data for body tissues, with data disk 1992.
[51] González SJ, Santa Cruz GA, Kiger III WS, Palmer MR, Busse PM, Zamenhof RG. NCTPlan, the new PC version of MacNCTPlan: improvements and verification of a BNCT treatment planning system. In: Sauerwein W, Moss RL, Wittig A, editors. Research and development in neutron capture therapy. Bologna, Italy: Monduzzi Editore; 2002. p. 556–7.
[52] Goorley JT, Kiger III WS, Zamenhof RG. Reference dosimetry calculations for neutron capture therapy with comparison of analytical and voxel models. Med Phys 2002;29:145–56.
[53] Laramore GE, Wheeler FJ, Wessol DE, Stelzer KJ, Griffin TW. A tumor control curve for malignant gliomas derived from fast neutron radiotherapy data: implications for treatment delivery and compound selection. In: Larsson B, editor. Proceedings of the 7th international symposium on neutron capture therapy for cancer. New York: Elsevier Science; 1997. p. 580–7.
[54] González SJ, Casal M, Pereira MD, Santa Cruz GA, Carando DG, Blaumann H, et al. Tumor control and normal tissue complications in BNCT treatment of nodular melanoma: a search for predictive quantities. Appl Radiat Isot 2009;67:S153–6.
[55] Suzuki M, Masunaga S, Kinashi Y, Takagaki M, Sakurai Y, Kobayashi T, et al. The effects of boron neutron capture therapy on liver tumors and normal hepatocytes in mice. Jpn J Cancer Res 2000;91:1058–64.
[56] Kiger JL, Kiger III WS, Riley KJ, Binns PJ, Patel H, Hopewell JW, et al. Functional and histological changes in rat lung after boron neutron capture therapy. Radiat Res 2008;170:60–9.
[57] Coderre JA, Hopewell JW, Turcotte JC, Riley KJ, Binns PJ, Kiger III WS, et al. Tolerance of normal human brain to boron neutron capture therapy. Appl Radiat Isot 2004;61:1083–7.
[58] Riley KJ, Binns PJ, Harling OK, Albritton JR, Kiger III WS, Rezaei A, et al. An international dosimetry exchange for BNCT Part II: computational dosimetry normalizations. Med Phys 2008;35:5419–25.
[59] Avoidance of radiation injuries from medical interventional procedures. Amsterdam: ICRP Publication; 2001.
[60] Archambeau JO, Ines A, Fajardo LF. Response of swine skin microvasculature to acute single exposures of X-rays: quantification of endothelial changes. Radiat Res 1984;98:37–51.
[61] Douglas BG. Implication of the quadratic cell survival curve and human skin radiation tolerance dose on fractionation and superfractionation dose selection. Int J Radiat Oncol Biol Phys 1982;8:1135–42.